RAD001 (Everolimus) Delays Tumor Onset and Progression in a Transgenic Mouse Model of Ovarian Cancer

Seiji Mabuchi,[1] Deborah A. Altomare,[1] Denise C. Connolly,[2] Andres Klein-Szanto,[3] Samuel Litwin,[4] Matthew K. Hoelzle,[1] Harvey H. Hensley,[5] Thomas C. Hamilton,[2] and Joseph R. Testa[1]

[1]Human Genetics Program, [2]Ovarian Cancer Program, [3]Department of Pathology, [4]Biostatistics Facility, and [5]Spectroscopy Support Facility, Fox Chase Cancer Center, Philadelphia, Pennsylvania

Abstract

The mammalian target of rapamycin (mTOR) is thought to play a critical role in regulating cell growth, cell cycle progression, and tumorigenesis. Because the AKT-mTOR pathway is frequently hyperactivated in ovarian cancer, we hypothesized that the mTOR inhibitor RAD001 (Everolimus) would inhibit ovarian tumorigenesis in transgenic mice that spontaneously develop ovarian carcinomas. We used Tg*MISIIR-TAg* transgenic mice, which develop bilateral ovarian serous adenocarcinomas accompanied by ascites and peritoneal dissemination. Fifty-eight female Tg*MISIIR-TAg* mice were treated with 5 mg/kg RAD001 or placebo twice weekly from 5 to 20 weeks of age. To monitor tumor development, mice were examined biweekly using magnetic resonance microimaging. *In vivo* effects of RAD001 on Akt-mTOR signaling, tumor cell proliferation, and blood vessel area were analyzed by immunohistochemistry and Western blot analysis. RAD001 treatment markedly delayed tumor development. Tumor burden was reduced by ∼84%. In addition, ascites formation, together with peritoneal dissemination, was detected in only 21% of RAD001-treated mice compared with 74% in placebo-treated animals. Approximately 30% of RAD001-treated mice developed early ovarian carcinoma confined within the ovary, whereas all placebo-treated mice developed advanced ovarian carcinoma. Treatment with RAD001 diminished the expression of vascular endothelial growth factor in tumor-derived cell lines and inhibited angiogenesis *in vivo*. RAD001 also attenuated the expression of matrix metalloproteinase-2 and inhibited the invasiveness of tumor-derived cells. Taken together, these preclinical findings suggest that mTOR inhibition, alone or in combination with other molecularly targeted drugs, could represent a promising chemopreventive strategy in women at high familial risk of ovarian cancer. [Cancer Res 2007;67(6):2408–13]

Introduction

Ovarian carcinoma is the fourth most common cause of cancer death among women in the United States (1). Due to the asymptomatic nature of early disease stages, ∼70% of cases have spread beyond the ovary at diagnosis and the cure rate for these patients is <20%. To improve survival, not only is there an urgent need to develop improved chemotherapeutic agents but also for novel chemoprevention strategies to prevent or delay disease progression. However, development of chemoprevention strategies for ovarian cancer has been delayed due, in part, to the lack of an appropriate experimental model. Recently, a transgenic mouse model of spontaneous epithelial ovarian cancer was developed by expression of SV40 Tag/tag under transcriptional control of the MISIIR promoter (2). Tumors arising in Tg*MISIIR-TAg* mice resemble poorly differentiated ovarian adenocarcinomas in women, frequently accompanied by malignant ascites and peritoneal spreading (2). SV40 Tag binds to and functionally inactivates p53 and Rb (3), which are frequently mutated in human ovarian cancer (4). SV40 tag binds protein phosphatase PP2A and inhibits its activity, resulting in activation of PI3K-AKT and mitogen-activated protein kinase (MAPK) signaling (3). Notably, AKT is frequently hyperactivated in human ovarian cancer (5). Moreover, expression of activated Akt in ovarian surface epithelial cells is sufficient to induce tumor formation in *p53*-null mice (6), suggesting that Akt is an important target for chemoprevention. Because elevated Akt activity results in hypersensitivity to mTOR inhibition (7), Tg*MISIIR-TAg-DR26* mice might serve as a valuable model to assess the chemopreventive potential of the mTOR inhibitor RAD001 (Everolimus). In this report, we show that RAD001 markedly delays tumor onset and progression in a mouse model of ovarian cancer.

Materials and Methods

Reagents. RAD001 and placebo were obtained from Novartis Pharma AG (Basel, Switzerland). Anti–phosphorylated (phospho)-p70S6K, anti-p70S6K, anti–phospho-AKT, anti-AKT, anti–phospho–mammalian target of rapamycin (mTOR), anti-mTOR, anti–phospho-GSK3, anti–cleaved caspase-3, and anti–matrix metalloproteinase (MMP) 2 antibodies were from Cell Signaling (Beverly, MA). Anti–vascular endothelial growth factor (VEGF), anti-SV40 Tag antibodies were from Santa Cruz Biotechnology (Santa Cruz, CA). Anti–β-actin was from Sigma (St. Louis, MO). Anti–MMP-2 antibody for immunohistochemistry was from Chemicon (Temecula, CA), and anti–CD31/platelet/endothelial cell adhesion molecule 1 (PECAM-1) from PharMingen (San Diego, CA).

Transgenic mice. The ovarian pathology of female Tg*MISIIR-TAg* founder mice has been described (2). A stably breeding transgenic line, Tg*MISIIR-TAg-DR26*, was established via an affected transgenic male founder. Transgenic female offspring develop bilateral epithelial ovarian carcinoma with complete penetrance, surviving an average of 143 days. Animal experiments were approved by our Institutional Animal Care and Usage Committee in accordance with NIH guidelines. Mice were typed for SV40 Tag by isolation of tail genomic DNA as described (2).

Drug preparation. RAD001 was formulated at 2% (w/v) in a microemulsion vehicle. For animal studies, RAD001 was diluted in double-distilled water just before administration by gavage. For *in vitro* analyses, RAD001 was prepared in DMSO.

Chemoprevention study. At 5 weeks of age, female Tg*MISIIR-TAg-DR26* mice were assigned to two groups receiving either RAD001 (*n* = 29) or placebo (*n* = 29). Treatment was given in 0.2 mL containing either 5 mg/kg

RAD001 or placebo twice weekly. Treatment was continued until 20 weeks of age, when all mice were euthanized. The size of ovaries was measured biweekly, using magnetic resonance microimaging (MRM). Weights were recorded weekly. At the time of sacrifice, mice were examined for peritoneal dissemination and ascites. Ovarian tumors and peritoneal implants were analyzed histologically. Final ovarian tumor volumes were calculated as follows: $V = L \times W \times D \times \pi/6$, wherein V is volume, L is length, W is width, and D is depth.

Magnetic resonance microimaging. MRM was done with a 7-Tesla vertical wide-bore magnet, using a Bruker DRX 300 spectrometer with a microimaging accessory. Mice were anesthetized by exposure to a mixture of oxygen and isofluorane (2%) for 10 min, after which the isofluorane concentration was reduced to 1%. Mice received a 0.2-mL gadolinium-diethyl-enetriaminepentaacetic acid injection of 10:1 diluted Magnevist (Berlex, Montville, NJ) contrast agent into the shoulder muscle immediately before scanning. Mice were positioned with the spine in the center of the image field of view. Images were made in sagittal and axial orientations with 0.5 mm slice thickness, 2.56 cm field of view, and 0.1 mm in-plane resolution, with four signal averages, and with 20 to 28 slices to cover the entire upper abdomen. Images acquired in Paravision were converted to Analyze format with the Bruker2analyze program. Tumor volumes were determined by outlining ovaries using the freeware program MRIcro.[6] Measured tumor volume was plotted against actual tumor volume at euthanasia. Linear regression analysis gave a correlation coefficient of 0.83 ($P < 0.01$).

Histologic analysis. Tumors were fixed in 10% neutral buffered formalin and embedded in paraffin. For immunohistochemistry, anti-SV40 TAg, anti–phospho-p70S6K (Thr[389]), anti–phospho-AKT (Ser[473]), anti–phospho-mTOR (Ser[2448]), anti–MMP-2, anti–CD31/PECAM-1, anti–Ki-67, and anti–cleaved caspase-3 were used. Surrounding nonneoplastic stroma served as an internal negative control. Staining was scored semiquantitatively, as described (8). Microvessel area was analyzed by anti-CD31 immunostaining (9).

Mouse ovarian carcinoma cell lines. Mouse ovarian carcinoma (MOVCAR) cell lines were obtained from ascites of Tg*MISIIR-TAg* mice (2). Cell lines were cultured at 37°C in DMEM containing 4% fetal bovine serum (FBS), 1% 1× insulin, transferrin, and selenium, penicillin (100 units/mL)/streptomycin (100 μg/mL), and 2 mmol/L glutamine in a humidified atmosphere of 5% CO_2.

Western blot analysis. Cell lines derived from ascites were treated with either DMSO (vehicle) or 20 nmol/L RAD001 for 0, 6, or 24 h. Cellular lysates and Western blots were prepared as described (10). Immunoblots were visualized with horseradish peroxidase–coupled goat anti–rabbit immunoglobulin or anti–mouse immunoglobulin using enhanced chemiluminescence (Perkin-Elmer, Boston, MA).

Cell proliferation assay. 3-(4,5-Dimethylthiazol-2-yl)-2,5-diphenyltetrazolium bromide (MTT) assay was used to analyze the effect of RAD001 on cell viability *in vitro* (10). Cells were cultured overnight in 96-well plates (10^4 per well). Cell viability was assessed by adding RAD001 at indicated concentrations for 72 h. The number of surviving cells was estimated by determining the $A_{490\ nm}$ of dissolved formazan product after addition of MTT for 1 h based on the manufacturer's instructions (Promega, Madison, WI). All experiments were carried out in quadruplicate, and viability is expressed as $A_{exp\ group}/A_{control} \times 100$.

In vitro cell invasion assay using matrigel. Invasiveness was analyzed using a BioCoat Matrigel Invasion Chamber kit (Becton Dickinson, Bedford, MA). Cells (2.5×10^4) with or without 20 nmol/L RAD001 in serum-free DMEM were seeded into transwell insert chambers containing a filter coated with Matrigel, and the insert chamber was placed in the lower compartment filled with DMEM with 4% FBS. Cells were incubated at 37°C in a 5% CO_2 atmosphere for 24 h. Cells that invaded the lower side of the filter were viewed microscopically and counted in random fields of view at ×200 magnification. Invasiveness was expressed as the mean cell number invading the lower side of the filter.

Statistical analysis. Body weight, tumor incidence, tumor volume, ascites formation, microvessel area, cell proliferation, and MOVCAR cell invasiveness were compared among RAD001-treated and control groups. Wilcoxon two-sample test was used to analyze body weight, tumor volume (estimated from MRM), and median time for tumors to reach 50 mm³. Fisher's exact test was used to analyze tumor incidence, ascites formation, microvessel area, cell proliferation, and invasiveness. $P < 0.05$ was considered significant.

Results

Because this mouse model expresses SV40 tag in ovarian epithelium (2), resulting tumor cells were expected to have activation of the Akt-mTOR pathway. At 9 to 14 weeks of age, some tumors were still confined within the ovary and strong immunoreactivity for Tag, phospho-Akt, phospho-mTOR, and phospho-p70S6K was detected (Fig. 1*A*), indicating that Akt-mTOR signaling is activated even in early ovarian lesions. Similar results were observed in more advanced tumors. Thus, Tg*MISIIR-TAg-DR26* mice were deemed a useful preclinical model to test the efficacy of RAD001 as an agent for early intervention/prevention of ovarian cancer.

To determine if RAD001 suppresses tumorigenesis, Tg*MISIIR-TAg-DR26* mice were treated with placebo or 5 mg/kg of RAD001 twice weekly. Because no obvious ovarian tumors were identified at 5 to 6 weeks of age in a pilot study of Tg*MISIIR-TAg-DR26* mice, treatment was started at 5 weeks and continued to 20 weeks of age. Body weight of RAD001-treated mice was ~10% lower than in placebo-treated mice (Supplementary Fig. S1), which was attributed to the large size of tumors in control mice. To rule out toxicity due to treatment with RAD001, a pathologist (A.K.S.) did a histologic assessment of various organs (liver, spleen, pancreas, kidney, small and large intestines, uterus, and ovaries) from seven RAD001-treated mice, and no toxic changes were observed.

Representative MRM images of ovarian tumors at 19 weeks of age and necropsy photos of the same mice at 20 weeks of age are shown in Fig. 1*B*. Figure 1*C* depicts time to tumor development based on MRM scans. Although nearly all mice developed ovarian tumors, RAD001 treatment significantly delayed tumor onset and progression. Median time for ovaries to reach a volume of 50 mm³ was 90 days in the placebo group compared with >122 days in RAD001-treated mice (Table 1). Median tumor burden measured at time of euthanasia was 429.2 mm³ in controls versus 26.2 mm³ in RAD001-treated mice; moreover, histologic analysis revealed early ovarian tumors confined within the ovary in 32% of RAD001-treated mice compared with 0% in controls.

Because ascitic fluid volume and size of disseminated tumors correlate with patient prognosis and contribute to patient malnutrition through loss of protein and/or suppressed appetite (11), it is important to control dissemination of tumors and ascites production. Ascites formation and peritoneal dissemination were detected in 73.9% of placebo-treated mice but only 21.4% in RAD001-treated mice (Table 1), demonstrating that RAD001 treatment during the early phase of spontaneous tumorigenesis significantly delays tumor development.

Rapamycin inhibits mTOR's ability to phosphorylate p70S6K and 4E-BP1, thereby inhibiting cell cycle progression of cancer cells (7). To investigate the mechanism by which RAD001 inhibits tumorigenesis in Tg*MISIIR-TAg-DR26* mice, we conducted cell proliferation assays using MOVCAR5 and MOVCAR6 cells. Proliferation was significantly inhibited by treatment with RAD001 in both lines (Fig. 2*A*). Treatment with 20 nmol/L RAD001 markedly decreased the number of Ki-67–positive cells and induced cleavage of PARP as

[6] http://www.psychology.nottingham.ac.uk/staff/cr1/mricro.html
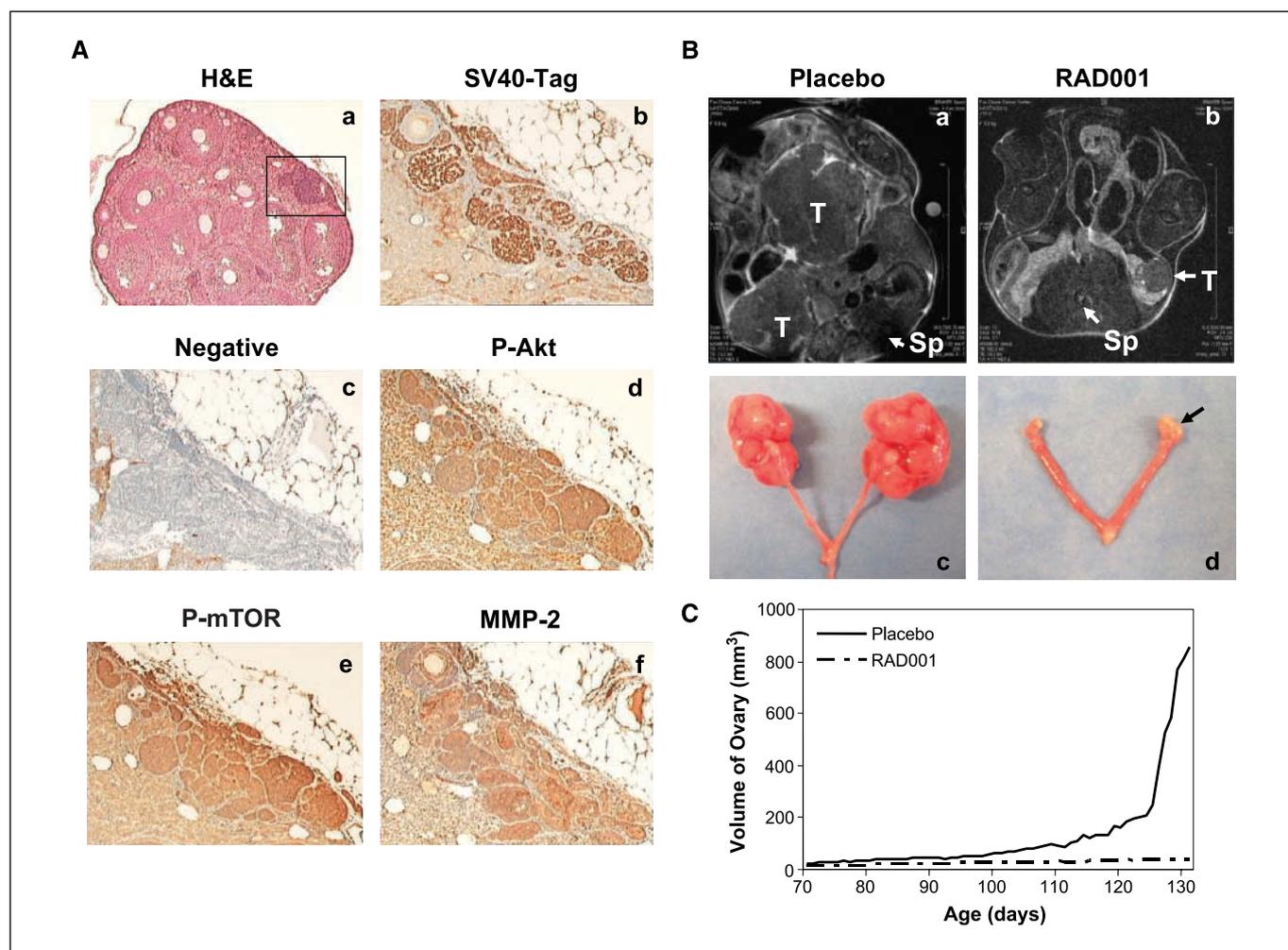
Figure 1. RAD001 inhibits ovarian tumorigenesis. *A,* the AKT-mTOR pathway is activated in early ovarian tumors from Tg*MISIIR-TAg-DR26* mice. Tissue sections were prepared for H&E staining (*a*) or immunohistochemical staining using anti–SV40 Tag (*b*), anti–phospho-Akt (*d*), anti–phospho-mTOR (*e*), and anti–MMP-2 antibodies (*f*). Negative control was incubated with phospho-Akt (Ser^{473}) antibody preabsorbed with a phospho-Akt blocking peptide (*c*). Representative fields. Magnification, ×100. *B,* representative MRM at 19 wks of age (*a, b*). Mice treated with placebo (*a*) or RAD001 (*b*) were scanned by MRM. Images have axial orientation. Tumor volume of the control mouse (*a*) was 720 mm^3 (right side of animal) and 1604 mm^3 (left side of animal) compared with 15 mm^3 (right side of animal) and 14 mm^3 (left side of animal) in the RAD001-treated mouse (*b*). *T,* ovarian tumor; *Sp,* spine. Autopsy photographs of ovarian tumors from the same mice after euthanization at 20 wks of age (*c, d*). *C,* inhibition of ovarian tumorigenesis in Tg*MISIIR-TAg-DR26* mice by RAD001. Tumor volume of individual mice was determined biweekly by MRM, and tumor volume was determined by manually outlining the ovaries using the software program MRIcro.

well (Supplementary Fig. S2). The apoptotic effect is noteworthy given that rapamycin can induce apoptosis in some settings (7). Immunostaining of tumor sections showed that RAD001 treatment results in a marked decrease in Ki-67–positive cells but only a modest increase in the number with immunoreactivity for cleaved caspase-3 (Supplementary Fig. S3). This suggests that RAD001 inhibits tumorigenesis in this model mainly by inhibiting cell proliferation rather than by inducing apoptosis.

As shown in Fig. 2*B*, Akt, mTOR, and p70S6K were phosphorylated in MOVCAR cells, indicating activation of Akt-mTOR signaling. Phosphorylation of p70S6K was significantly decreased by RAD001 treatment, indicating inhibited downstream signaling of mTOR. Similarly, ovarian tumors from RAD001-treated mice showed markedly decreased phospho-p70S6K staining (Supplementary Fig. S4). Western blotting and immunohistochemistry revealed that RAD001 does not affect expression of SV40 Tag (Supplementary Fig. S5).

VEGF is known to stimulate tumor angiogenesis and mediate ascites formation (12). Because rapamycin can decrease expression of VEGF in ovarian tumors (13), we tested whether RAD001 affects the expression of VEGF in MOVCAR cells (Fig. 2*C*). VEGF expression was found to be significantly inhibited by RAD001 in both tested MOVCAR lines.

To examine if RAD001 inhibits angiogenesis *in vivo*, distribution of the endothelial marker CD31 was assessed by immunohisto-chemistry (Fig. 3*A*). Large CD31-immunopositive vessels were observed in tumors from placebo-treated mice, whereas fewer and smaller vessels were observed in tumors from RAD001-treated mice. There was a significant decrease of microvessel area in RAD001-treated tumors compared with control tumors (Fig. 3*B*). Thus, RAD001's antitumor effect may be associated, in part, with inhibition of angiogenesis.

MMP-2 expression is an early event in the invasiveness of ovarian carcinoma (14). Elevated MMP-2 expression is associated with tumor invasiveness and metastatic potential, ascites formation, peritoneal dissemination, and poor prognosis in patients with ovarian cancer (14, 15). We found that MMP-2 is expressed in early ovarian tumors from our mice (Fig. 1*A*). MMP-2 expression was observed in both tested MOVCAR lines, and treatment with

Table 1. Effect of RAD001 on tumor development in a mouse model of ovarian cancer

Treatment	No. mice	No. mice with tumors (%)	No. mice with advanced tumors (%)	No. mice with early tumors (%)	Tumor volume (mm^3)		Median time for tumor to reach 50 mm^3 (d)	Incidence of ascites formation (%)	Tumor type	Incidence of ascites formation (%)
					Median	Mean				
Placebo	29	29 (100)	29 (100)	0 (0)	429.2	551.5	90	73.9	Advanced	73.90
									Early tumor	0
RAD001	29	28 (96.6)	19 (67.9)*	9 (32.1)*	26.2*	91.4*	>122	21.4*	Advanced	31.6*
									Early tumor	0

*Significantly different from placebo group (*P* < 0.01).

RAD001 significantly attenuated expression of MMP-2 (Fig. 2*D*) and inhibited cell invasion through Matrigel (Fig. 3*C, D*). These findings are consistent with the fact that RAD001 inhibits tumor dissemination and ascites production in Tg*MISIIR-TAg-DR26* mice.

Discussion

Our data show that mTOR inhibition markedly delays tumorigenesis in a murine model of ovarian cancer. Although RAD001 treatment did not reduce tumor incidence, it resulted in a remarkable reduction in the number of mice with advanced disease and inhibited ascites formation and peritoneal dissemination. These findings have important implications, because the cure rate of patients with early ovarian cancer is nearly 90% compared with <20% in patients with advanced disease (16).

However, some tumors in RAD001-treated mice escaped the inhibitory effect of RAD001 and became large, indicating the presence of an alternative proliferation pathway. Germane to this, recent work indicates that a combination of rapamycin and a MAPK inhibitor is necessary to inhibit the growth of ovarian tumors that have two redundant proliferation signals (i.e., mTOR and MAPK; ref. 17). In MOVCAR cells, both Akt-mTOR (Fig. 2*B*) and MAPK pathways (Supplementary Fig. S6) are activated, likely due to the expression of SV40 tag. Therefore, treatment with RAD001 and a MAPK inhibitor might be more efficacious in RAD001-resistant Tg*MISIIR-TAg-DR26* tumors.

Another possible reason why some tumors escaped the inhibitory effect of RAD001 is that drug treatment may have stimulated a survival pathway. Although RAD001 effectively inhibited phosphorylation of p70S6K, phosphorylation of Akt (as well as mTOR and GSK3) was up-regulated by RAD001 treatment in MOVCAR cells and tumors (Fig. 2*B*; Supplementary Fig. S4). This is consistent with recent work demonstrating that mTOR inhibition triggers a feedback mechanism that activates Akt, which can then activate other downstream pathways that may promote tumor growth (18). Thus, future studies are planned to evaluate the chemopreventive efficacy of RAD001 combined with a PI3K/Akt inhibitor using Tg*MISIIR-TAg-DR26* mice.

Figure 2. RAD001 inhibits mTOR activity and cell proliferation. *A*, effect of RAD001 on proliferation of MOVCAR cells. MOVCAR cell lines were treated either with DMSO (*Control*) or indicated concentrations of RAD001 in the presence of 4% FBS for 72 h. Cell viability was assessed by MTT assay. *B*, effect of RAD001 on Akt-mTOR signaling. Cells were treated with either DMSO or 20 nmol/L RAD001 for 6 h in the presence of 4% FBS. Western blots were screened with antibodies against the indicated proteins. All are from the same membrane and an 8% gel, except for phospho-mTOR and mTOR which are from a separate 6% gel. *C*, *in vitro* effects of RAD001 on expression of VEGF in MOVCAR cells. The cells were treated with 20 nmol/L of RAD001 for 24 h in the presence of 4% FBS, and the effect of RAD001 on the expression of VEGF was determined by immunoblotting. *D*, effect of RAD001 on expression of MMP-2 in MOVCAR cells. Cells were treated with 20 nmol/L RAD001 for 24 h in the presence of 4% FBS, and the effect of RAD001 on the expression of MMP-2 was determined by Western blotting. Actin was used as a loading control in (*B–D*).
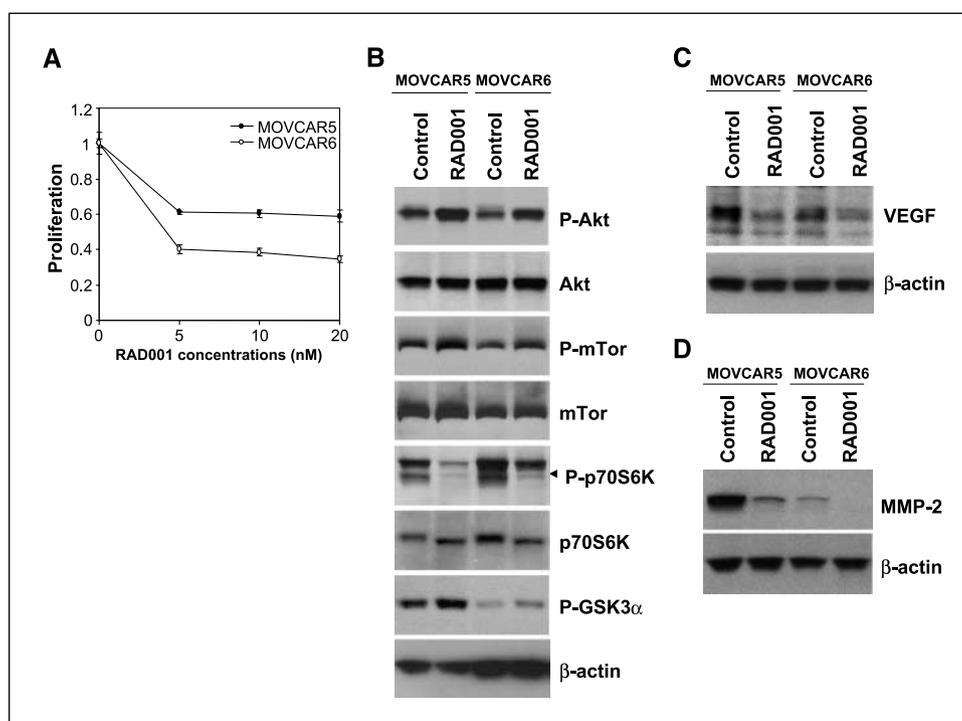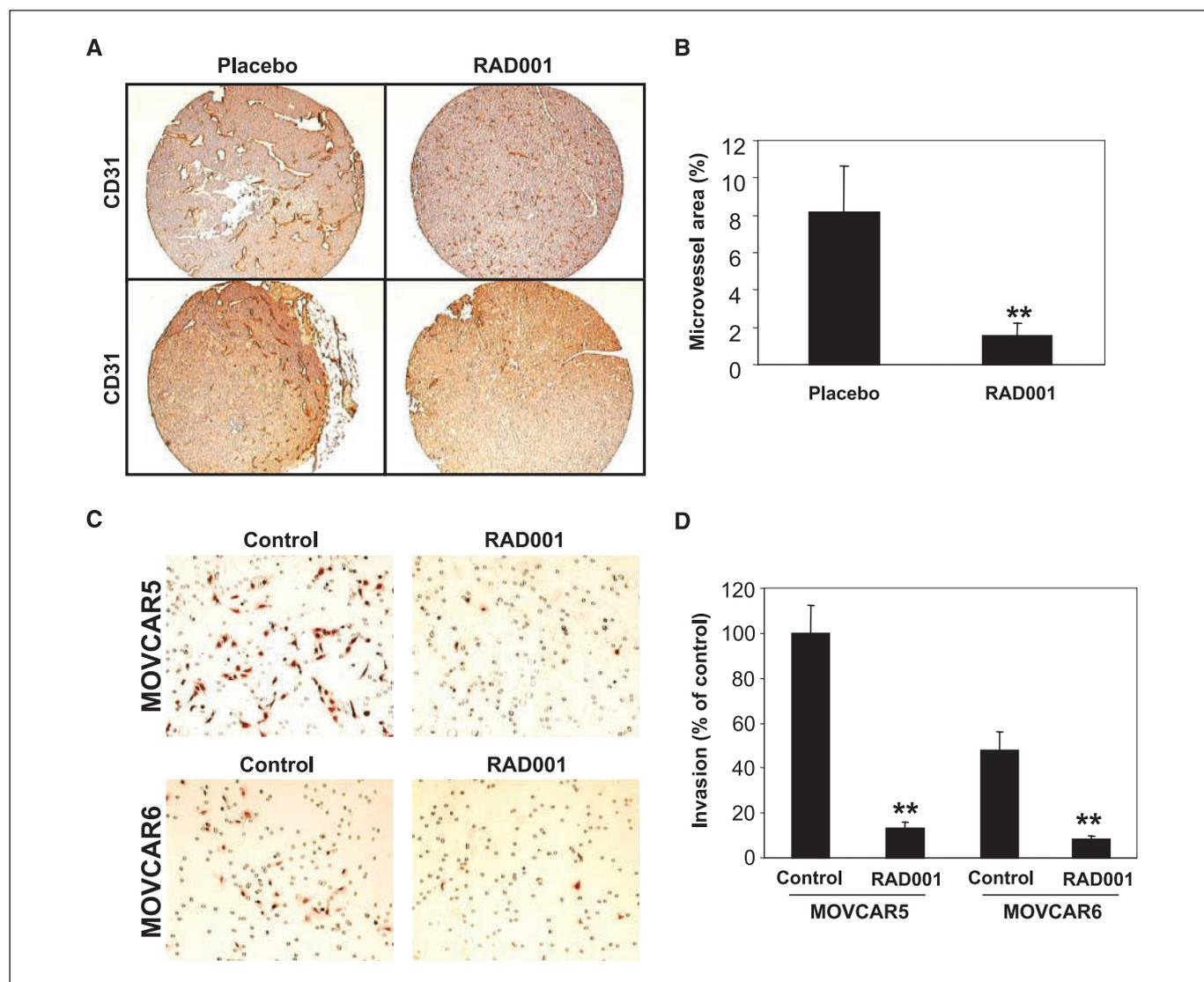
Figure 3. RAD001 inhibits angiogenesis and invasiveness. *A,* immunohistochemical staining of representative ovarian carcinomas from Tg*MISIIR-TAg* transgenic mice. Serial sections of an ovarian cancer tissue microarray were stained with anti–CD31/PECAM-1 antibody. Magnification, ×50. *B,* histogram indicating microvessel area of individual ovarian tumors analyzed by anti-CD31 immunostaining. Significant differences are indicated by asterisks (**, $P < 0.01$). *C,* effect of RAD001 on invasiveness of MOVCAR cells. The cells were seeded on Matrigel-coated filters, treated with 20 nmol/L of RAD001, and incubated for 24 h. Magnified views of undersides of filters are shown. *D,* histogram depicting the relative number of cells that penetrated through the Matrigel, with the number of penetrating cells in the vehicle control set arbitrarily at 1.0 (100%). *Columns,* mean from at least three separate experiments; *bars,* SE. Significant differences are indicated by asterisks (**, $P < 0.01$).

Chemoprevention will likely require long-term treatment. Thus, a low toxicity profile is required for an effective chemopreventive agent. RAD001 is approved in Europe as an immunosuppressive agent in the solid organ transplantation setting, and there are extensive safety data regarding long-term usage of RAD001 (19). The dosage used in our study seemed to be well tolerated, with no toxic changes evident histologically.

The risk of developing ovarian cancer is 30% to 60% in women with *BRCA1* mutations and 10% to 30% in those with *BRCA2* mutations. Currently, prophylactic oophorectomy is the only way to reduce lifetime risk of ovarian cancer in these women (20). Whereas there is no clearly defined ovarian preneoplastic lesion, phospho-AKT/phospho-mTOR immunostaining is frequently found in inclusion cysts and other histologic lesions in ovaries removed prophylactically from women with hereditary *BRCA1* or *BRCA2* mutations.[7] Collectively, our findings suggest that mTOR inhibition might be a useful strategy to prevent or delay onset of ovarian cancer in women with hereditary ovarian cancer syndrome.

Acknowledgments

---

[7] Unpublished data.

References

1. Jemal A, Murray T, Ward E, et al. Cancer statistics, 2005. CA Cancer J Clin 2005;55:10–30.
2. Connolly DC, Bao R, Nikitin AY, et al. Female mice chimeric for expression of the simian virus 40 TAg under control of the MISIIR promoter develop epithelial ovarian cancer. Cancer Res 2003;63:1389–97.
3. Arroyo JD, Hahn WC. Involvement of PP2A in viral and cellular transformation. Oncogene 2005;24:7746–55.
4. Gallion HH, Pieretti M, DePriest PD, van Nagell JR, Jr. The molecular basis of ovarian cancer. Cancer 1995;76:1992–7.
5. Altomare DA, Wang HQ, Skele KL, et al. AKT and mTOR phosphorylation is frequently detected in ovarian cancer and can be targeted to disrupt ovarian tumor cell growth. Oncogene 2004;23:5853–7.
6. Orsulic S, Li Y, Soslow RA, Vitale-Cross LA, Gutkind JS, Varmus HE. Induction of ovarian cancer by defined multiple genetic changes in a mouse model system. Cancer Cell 2002;1:53–62.
7. Bjornsti MA, Houghton PJ. The TOR pathway: a target for cancer therapy. Nat Rev Cancer 2004;4:335–48.
8. Wang HQ, Altomare DA, Skele KL, et al. Positive feedback regulation between AKT activation and fatty acid synthase expression in ovarian carcinoma cells. Oncogene 2005;24:3574–82.
9. LeBlanc R, Catley LP, Hideshima T, et al. Proteasome inhibitor PS-341 inhibits human myeloma cell growth *in vivo* and prolongs survival in a murine model. Cancer Res 2002;62:4996–5000.
10. Mabuchi S, Ohmichi M, Nishio Y, et al. Inhibition of NFκB increases the efficacy of cisplatin in *in vitro* and *in vivo* ovarian cancer models. J Biol Chem 2004;279:23477–85.
11. Roszkowski P, Wronkowski Z, Szamborski J, Romejko M. Evaluation of selected prognostic factors in ovarian cancer. Eur J Gynaecol Oncol 1993;14 Suppl:140–5.
12. Yoneda J, Kuniyasu H, Crispens MA, et al. Expression of angiogenesis-related genes and progression of human ovarian carcinomas in nude mice. J Natl Cancer Inst 1998;90:447–54.
13. Skinner HD, Zheng JZ, Fang J, Agani F, Jiang BH. Vascular endothelial growth factor transcriptional activation is mediated by hypoxia-inducible factor 1α, HDM2, and p70S6K1 in response to phosphatidylinositol 3-kinase/AKT signaling. J Biol Chem 2004;279:45643–51.
14. Torng PL, Mao TL, Chan WY, Huang SC, Lin CT. Prognostic significance of stromal metalloproteinase-2 in ovarian adenocarcinoma and its relation to carcinoma progression. Gynecol Oncol 2004;92:559–67.
15. Stack MS, Ellerbroek SM, Fishman DA. The role of proteolytic enzymes in the pathology of epithelial ovarian carcinoma. Int J Oncol 1998;12:569–76.
16. Paley PJ. Ovarian cancer screening: are we making any progress? Curr Opin Oncol 2001;13:399–402.
17. Coltella N, Rasola A, Nano E, et al. p38 MAPK turns hepatocyte growth factor to a death signal that commits ovarian cancer cells to chemotherapy-induced apoptosis. Int J Cancer 2006;118:2981–90.
18. O'Reilly KE, Rojo F, She QB, et al. mTOR inhibition induces upstream receptor tyrosine kinase signaling and activates Akt. Cancer Res 2006;66:1500–8.
19. Kreis H, Oberbauer R, Campistol JM, et al. Rapamune Maintenance Regimen Trial. Long-term benefits with sirolimus-based therapy after early cyclosporine withdrawal. J Am Soc Nephrol 2004;15:809–17.
20. Kauff ND, Satagopan JM, Robson ME, et al. Risk-reducing salpingo-oophorectomy in women with a BRCA1 or BRCA2 mutation. N Engl J Med 2002;346:1609–15.

RAD001 (Everolimus) Delays Tumor Onset and Progression in a Transgenic Mouse Model of Ovarian Cancer

Seiji Mabuchi, Deborah A. Altomare, Denise C. Connolly, et al.

Updated version	Access the most recent version of this article at: http://cancerres.aacrjournals.org/content/67/6/2408
Supplementary Material	Access the most recent supplemental material at: http://cancerres.aacrjournals.org/content/suppl/2007/03/19/67.6.2408.DC1

Cited articles	This article cites 19 articles, 6 of which you can access for free at: http://cancerres.aacrjournals.org/content/67/6/2408.full#ref-list-1
Citing articles	This article has been cited by 27 HighWire-hosted articles. Access the articles at: http://cancerres.aacrjournals.org/content/67/6/2408.full#related-urls

E-mail alerts	Sign up to receive free email-alerts related to this article or journal.
Reprints and Subscriptions	To order reprints of this article or to subscribe to the journal, contact the AACR Publications Department at pubs@aacr.org.
Permissions	To request permission to re-use all or part of this article, use this link http://cancerres.aacrjournals.org/content/67/6/2408. Click on "Request Permissions" which will take you to the Copyright Clearance Center's (CCC) Rightslink site.